KFKI-73-19

L. Koblinger

MONTE CARLO CALCULATIONS ON CHEST X-RAY EXAMINATIONS. RESULTS FOR MONOENERGETIC BEAMS

Hungarian Academy of Sciences

CENTRAL RESEARCH INSTITUTE FOR PHYSICS

BUDAPEST

KFKI-73-19

MONTE CARLO CALCULATIONS ON CHEST X-RAY EXAMINATIONS. RESULTS FOR MONOENERGETIC BEAMS

L. Koblinger

Health Physics Department
Atomic Energy Division

Central Research Institute for Physics, Budapest, Hungary

ABSTRACT

Some important quantities, like the dose absorbed in internal organs, are in practice not measurable during diagnostic X-ray examinations. This paper aims to demonstrate how the introduction of Monte Carlo calculation techniques into diagnostical studies can help in their determination. After a short description of the principles of method and a computer code which was developed for the purpose some results of relevance to chest radiography are presented. The patient is represented by the inhomogeneous Snyder phantom, while the X-ray source is simulated by a parallel beam of photons. The spectra of both the image-forming and backscattered photons and the doses absorbed in the different organs are determined, for discrete initial energies from 25 up to 150 keV. Comments on the contrast of the X-ray image are also included.

KIVONAT

A diagnosztikai mellkas-átvilágitások során több olyan fontos jellemző, mint például a belső szervekben elnyelt dózis mérése gyakorlatilag megoldhatatlan. A jelen dolgozatban szeretnénk rávilágitani, hogy egyes jellemzők meghatározásában a Monte Carlo számitások milyen nagy segitséget nyujthatnak.

A módszer és egy erre a célra irt számitógépi program ismertetése után mellkas-átvilágitásra vonatkozó eredményeket közlünk. A vizsgált személyt az inhomogén Snyder-fantommal, a forrást pedig párhuzamos monoenergiás /25-150 keV/ foton nyalábbal modelleztük. Meghatároztuk az egyes szervekben elnyelt dózist, valamint a képalkotó és a visszavert fotonok spektrumát. A röntgenkép kontrasztját is tanulmányoztuk.

РЕЗЮМЕ

При диагностической рентгеноскопии грудной клетки, существует несколько таких характеристических показателей, как например, доза, поглощенная внутренними органами, измерение которых практически неразрешимо. В настоящей статье мы хотели бы осветить то, какую большую помощь оказывают вычисления Монте Карло, при определении некоторых характеристик.

После изложения метода и, написанной для этой цели, программы для вычислительной машины, мы сообщаем результаты, касающиеся рентгеноскопии грудной клетки. Исследуемую личность мы моделировали с помощью неоднородного Снайдер--фантома, а источник - с помощью параллельного моноэнергетического /25··150 кэв/ фотонного пучка. Мы определили дозу, поглощенную отдельными органами, и кроме того спектр фотонов, образующих изображение и спектр отраженных фотонов. Мы занимались также и изучением контраста рентгенограммы.

1. INTRODUCTION

Nowadays most people undergo a radiographic exposure at least once in three or four years. Though these examinations are very useful from the diagnostic point of view, they may be harmful because of the effects of the ionizing radiation. There is thus a permanent inducement to lower the dose received by the patient while at the same time improving - or at least not impairing - the quality of the image. These two aims are difficult to reconcile, since in most cases, for a given technique, an improvement of the image /e.g. by use of grids/ has to be paid for by a higher absorbed dose. Radiologists have therefore to be very careful in choosing the proper technique, the peak voltage of the X-ray tube and the filtration of the beam.

The in vivo measurement of dose is also hedged with difficulties, especially in the case of internal organs /e.g. heart or lungs/ where the placing of dosimeters is out of the question. We should like in this paper to advocate the use of Monte Carlo method for the calculation of dose received during diagnostic examinations. These calculations have their own limitations and inaccuracies, but they can supply new information that - taken together with experimental data - would be of considerable help to radiologists.

Here the Monte Carlo method itself and the model on which it operates are described and illustrated by results referring monoenergetic incident beams.

2. MONTE CARLO METHOD

The problem is the following: photons penetrate an inhomogeneous phantom whose organs are defined by relatively complicated expressions, and we wish to determine both the dose absorbed in the different organs as well as the spectrum of the transmitted and the backscattered photons. The only feasible approach to a situation of this complexity is Monte Carlo computation, which is nowadays a well-established method, amongst other things precisely through its frequent use in dose calculations.

In essence, the Monte Carlo computation traces the path of a photon step by step, simulating the successive interactions between the photon and the intervening matter and calculating the energy released at each interaction site. In our calculation the energy released is assumed to be absorbed

at the same point /i.e. the kerma is equal to the absorbed dose/.

Step 1. A photon enters the phantom. Its site of entry and direction of flight are chosen randomly in accordance with the spatial distribution of the source photons, and its energy in accordance with the source energy distribution. /Naturally, if e.g. a monoenergetic source is used, then this last selection is replaced by a simple assignment./ The incident photon receives an initial statistical weight $w_1 = 1$.

Steps 2 - 4. For path length selection in the inhomogeneous phantom the special technique proved by Coleman /1968/ is used.

Step 2. A free path length is chosen from exponentially distributed random numbers. The mean value of these numbers is the mean free path length $L = 1/\mu_{max}$, where μ_{max} is the maximum of the linear attenuation coefficients of all the tissues /in our phantom calculations μ_{max} always refers to the skeletal tissue/.

Step 3. A potential collision site is determined from the previous collision site, the direction of flight and the path length.

Step 4. The organ in which the potential collision site lies is ascertained.

If the photon left the body and cannot re-enter, then the procedure resumes at step 7. An internal void or concavity can be regarded as an "organ" with zero cross section.

If, for the organ in question, $\mu = \mu_{max}$, the potential collision site is regarded as a real one, and the procedure continues with step 5. If, however, $\mu < \mu_{max}$, then a random number uniformly distributed between 0 and 1 is choosen, and provided this number is less than μ/μ_{max}, the potential site is again regarded as a real one; otherwise, the procedure is repeated from step 2, but this time the new path length is added to the last potential collision site.

Step 5. A new energy and direction are chosen on the basis of the Klein-Nishina differential cross-section formula. Absorption due to photoelectric interaction is simulated by reduction of the statistical weight, the weight after the nth collision being

$$w_n = w_{n-1} \cdot \left(1 - \frac{\mu_p}{\mu}\right)$$

where μ_p is the attenuation coefficient for the photoelectric process.

If the photon's energy or its weight falls below a given limit /5 keV and 10^{-4} in our calculations/, then the entire energy $w_{n-1} \cdot E_{n-1}$ of the photon is assumed to be absorbed at the collision site, and the procedure is repeated from step 1.

Step 6. The energy deposited during the nth interaction is

$$E_{dep} = w_{n-1}\left[\frac{\mu_\rho}{\mu} E_{n-1} + (1-\frac{\mu_\rho}{\mu})(E_{n-1}-E_n)\right].$$

This energy deposition is added to the energy previously absorbed in the organ in which this collision site lies.

The process is continued from step 2.

Step 7. When the photon leaves the body, it is ascertained whether it crosses any external surface of interest /e.g. the photoreceptor plane/; if so, the statistical weight of the photon is added to the content of the storage element appropriate to its energy. By this method the spectrum of the photons reaching a given plane can be determined. After this step the whole simulation is repeated from the beginning.

During the accumulation of the absorbed energy the square of the energy deposited in a given organ by one photon is also stored for the calculation of the standard deviation. If E_i is the energy deposited by all interactions of the i^{th} photon in the organ of interest, and E and σ are the mean value and standard deviation of the E_i-s, the coefficient of variation of $\bar{E}$/i.e. the quantity characterising the statistical uncertainty / is then $CV = \sigma/\bar{E}$.

3. THE PHANTOM

To calculate the dose absorbed in the various organs the inhomogeneous phantom described by Snyder, Ford, Warner and Fisher /1969/ is used. This phantom /Fig.1/ has a total volume of about 70 dm^3 and is divided into three main regions - head, trunk and legs. It comprises 23 internal organs each of which is defined by a quadratic equation /the brain, for example is a simple ellipsoid, while the heart is a half ellipsoid capped by a hemisphere which is cut by a plane/. The phantom is inhomogeneous, as the lungs and the skeleton have elemental compositions and densities differing from the remaining tissues.

For the calculations we developed a computer code -DISDOS- written for determination of the absorbed dose due to different external photon sources /Koblinger, 1971/. The elemental compositions of the tissues can be individually specified in the input of the code, though it has been established that the slight discrepancies in the data published by different authors have no important effect on the absorbed dose /Koblinger 1972/. The compositions and densities used in this study for the three different kinds of tissue are given in Table 1. The cross sections used for the calculations are taken from the tables of Hubbell /1969/.

4. CALCULATIONS FOR MONOENERGETIC PARALLEL BEAM

4.1 THE MODEL

The simplest model of an X-ray examination is illustrated in Fig.1. A parallel beam of photons enters the body from the back, as the patient is assumed to be examined p.a. The irradiated surface is a parallelogram with an area of 856.8 cm^2 /this covers the lungs and the upper nine ribs/ on which the photons are uniformly distributed. In this first approximation of the problem only photons from a monoenergetic source are considered; this is not a limitation, since the results for any given incident spectrum can be obtained by linear combination of its component monoenergetic values. Backscattered radiation is detected by a circular detector /314 cm^2/ placed behind the patient's back. The photoreceptor is located just in front of the patient's chest and has the same shape and dimensions as the irradiated area.

To study the contrast of the image the photoreceptor area is divided into two parts

1/ the projection of the intercostal region, and
2/ the area shadowed by the ribs or the spine /or both/.

The spectra of photons are obtained both for the whole image and for the second part of the photoreceptor /simple subtraction gives the spectrum for the first part/.

The uncollided photons are handled separately during the determination of the spectrum of photons which pass through the receptor to enable study of the contrast-improving effect of Bucky grids, as an idealized grid would absorb all of the scattered photons and so only the uncollided photons would form the image.

The incident energy ranges from 25 to 150 keV.

4.2 SPECTRA OF TRANSMITTED AND BACKSCATTERED PHOTONS

The photons crossing either the photoreceptor area or the circular detector are allocated to 5 keV wide energy groups. The spectra of both the image-forming and the backscattered photons for 50, 75, 100, 125 and 150 keV incident energies are given in Fig.2.

The energy distribution of the backscattered photons throws light on an important question. Quite frequently, the incident exposure is measured by placing a detector /e.g. an ion chamber/ between the X-ray source and the patient. This chamber will detect not only the incident photons but a fraction of the backscattered photons, too, and this error /or overestimation/ is

the largest when the detector is placed close to the patient. In Fig. 3 one can see that the exposure due to the backscattered photons may, in the vicinity of the centre of the irradiated area, be as high as 22% of the exposure due to the primary radiation.

4.3 CONTRAST

To characterize the contrast of the X-ray image, the term exposure ratio is introduced in the following manner: By separately counting the photons reaching the two areas of the photoreceptor, the photon energy distribution and from this - with the aid of the appropriate $R.cm^2$/photon conversion factors /Fitzgerald, Brownell and Mahoney, 1967/ - the average exposure on each area can be calculated. The ratio of the exposures on the intercostal and bone-shadowed areas is then the exposure ratio.

Plots of the exposure and exposure ratio vs. incident photon energy are presented in Fig.4. The second set of curves refers to the case when only the uncollided photons are detected. The exposure on the receptor is always a monotonously increasing function of the energy, while the exposure ratio is a monotonously declining curve. The slopes of the curves are greater at lower energies, where the nuclear cross section itself changes faster because of the photoelectric process.

The contribution of the uncollided photons to the total exposure is about 40-50 per cent.

4.4 THE ABSORBED DOSES

The energy quanta deposited in the collisions are stored separately during the calculation for each of the 23 organs and the absorbed energy is summed up for the gastro-intestinal tract /stomach + small intestine + large intestine/ and the skeleton /legs + arms + pelvis + spine + skull + ribs/ as well as for the three main regions of the body /head, trunk and legs/ and for the whole body. Plots of the absorbed dose vs. photon energy for some of the organs and body parts are given in Figs. 5 and 6. The dose values are normalized to one incident photon.

The highest dose occurs in the lungs and ribs, which lie directly in the path of beam. It should be noted, however, that only the upper nine of the twelve ribs are irradiated directly and that - especially at lower photon energies - the dose in the dorsal half cage, where most of the beam attenuation takes place, may be twice or more the average values given in fig.5. At low energies nearly a fifth of the whole absorbed energy is deposited in the ribs /see Fig. 7/, but this fraction decreases rapidly at higher energies.

The lungs absorb 7-8 per cent of the total absorbed energy - almost independently of the incident photon energy. The heart, although it lies in the direct beam, is relatively far from the body's surface, therefore at low energies, where the mean free path length of the photons is small, it absorbs a much lower dose than the ribs or lungs. The same strong energy dependence is seen for the organs /or body parts/ which lie out of the direct beam.

In Fig. 6 the dose curves for some more problematic cases are drawn. The total dose to the bone marrow in the phantom was calculated on the assumption that in the skull this tissue receives 20 per cent of the absorbed energy, in the arm bones 30 per cent, in the leg bones and ribs 40 per cent, in the pelvis 45 per cent, and in the spine 50 per cent. Of course, this simple method can give only approximate values.

The dose absorbed by the skin, which is treated as a uniform two-millimeter thick layer on the body surface, may obviously be much higher in the area where the photons enter the body than the average values shown in the figure /the ratio of irradiated per whole surfaces is 1:15/. Similarly, as somewhat less than half of the length of the whole spine /25.2 of the total 56.5 cm/ is irradiated directly, the dose in this section may exceed the average values presented by a factor of more than two.

For such organs as the kidney or the spleen the statistical uncertainty is fairly high, but at least the shape and the position of the curve are obvious. For the thymus and the thyroid the coefficients of variation are about 25-30 and 50% respectively, so the curves presented can be regarded as rough estimations only and there is no sense in plotting the single points.

The gonads, unfortunately, are too small and lie too far from the beam for Monte Carlo calculations to give accurate results within a reasonable running time.

5. CONCLUSIONS

The results presented above demonstrate that the Monte Carlo method can make important contributions to the study of diagnostic examinations. It can provide data on such things as the spectrum of the image-forming photons or the dose vs. incident photon energy curves for internal organs which are almost non-existent in the literature but which may be very useful for further calculations and in design of radiographic appliances.

Further results based on this technique and partly on these calculations will be presented in the Journal of Physics in Medicine and Biology.

REFERENCES

Coleman, W.A., 1968, Nucl. Sci. Eng., 32, 76-81.

Fitzgerald, J.J., Brownell, G.L., and Mahoney, F.J., 1967, Mathematical Theory of Radiation Dosimetry /New York: Gordon and Breach/ p. 228.

Hubbell, J.H., 1969. Photon Cross Sections, Attenuation Coefficients, and Energy Absorption Coefficients from 10 keV to 100 GeV /National Bureau of Standards Report NSRDS-NBS 29/.

Koblinger, L., 1971, Two Codes for Calculation of Dose Distribution in Human Phantoms Irradiated by External Photon Sources /Central Research Institute for Physics Report KFKI-71-12/.

Koblinger, L., 1972. Acta Biochim. et Biophys. Acad. Sci. Hung., 7, 189-192.

Snyder, W.S., Ford, M.R., Warner, G.G., and Fisher, H.L., 1969, MIRD Pamphlet No. 5. J. Nucl. Med. 10, Supplement 3.

TABLE 1.

Elemental compositions and densities for the three kinds of tissue

Element	Composition /in weight %/ for the		
	bone	lung	remaining
	tissues		
1 H	7.04	10.21	10.48
6 C	22.82	10.01	23.03
7 N	3.87	2.80	2.33
8 O	48.62	76.00	63.23
11 Na	0.32	0.19	0.13
15 P	6.95	0.08	0.24
16 S	0.17	0.23	0.22
17 Cl	0.14	0.27	0.14
19 K	0.15	0.20	0.20
20 Ca	9.92	0.01	--
density (g/cm^3)	1.5	0.3	1.0

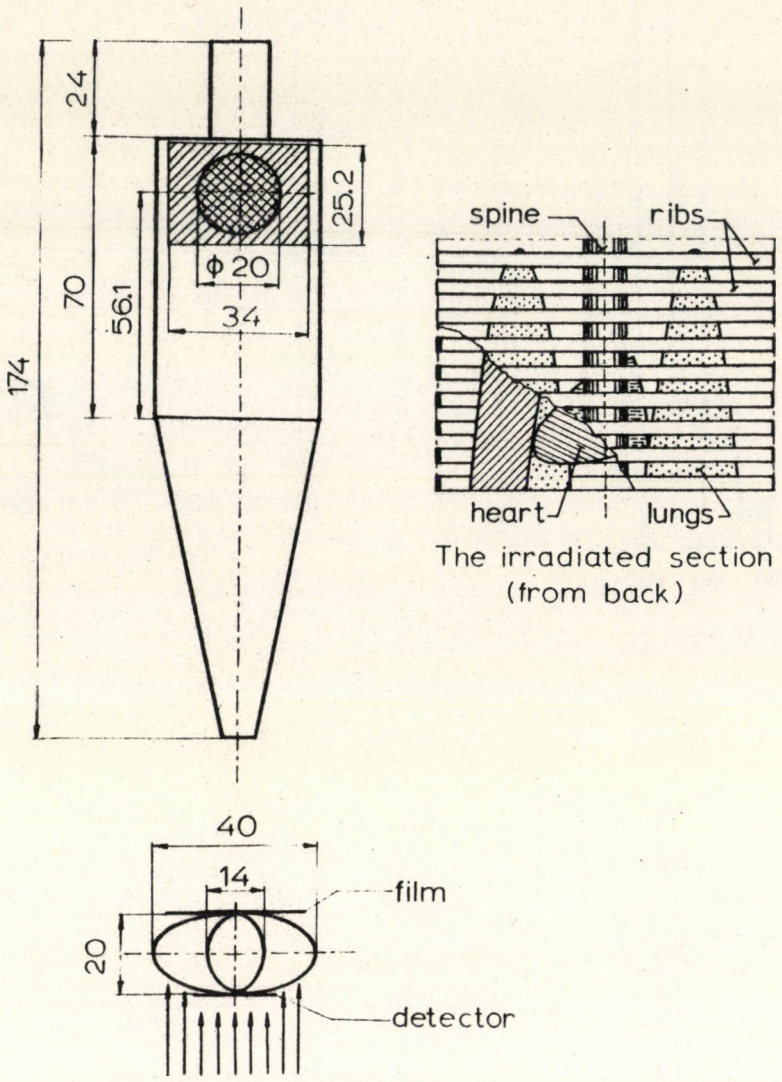

Fig. 1

The shape of the Snyder phantom, the circumstances of the examinations, and the section of the directly irradiated part of the body

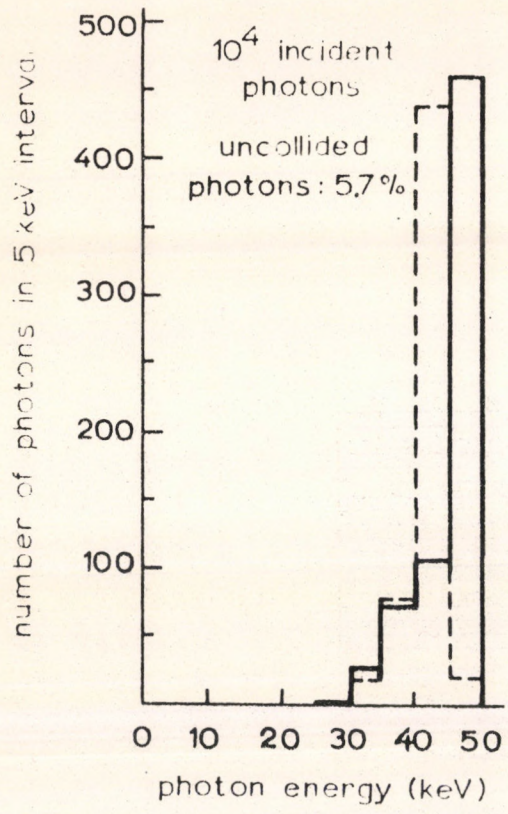

a/

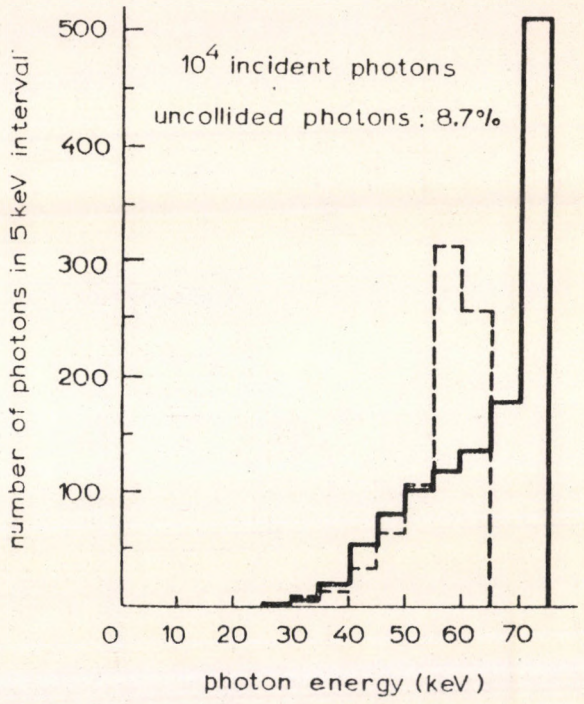

b/

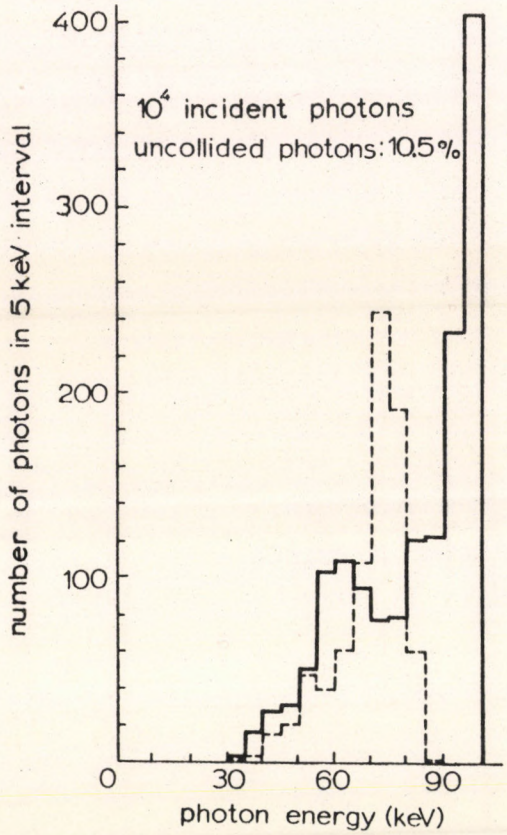

c/

Fig. 2

Spectra of the image-forming /full lines/ and backscattered /dashed lines/ photons for incident photon energies of /a/ 50; /b/ 75; /c/ 100 keV

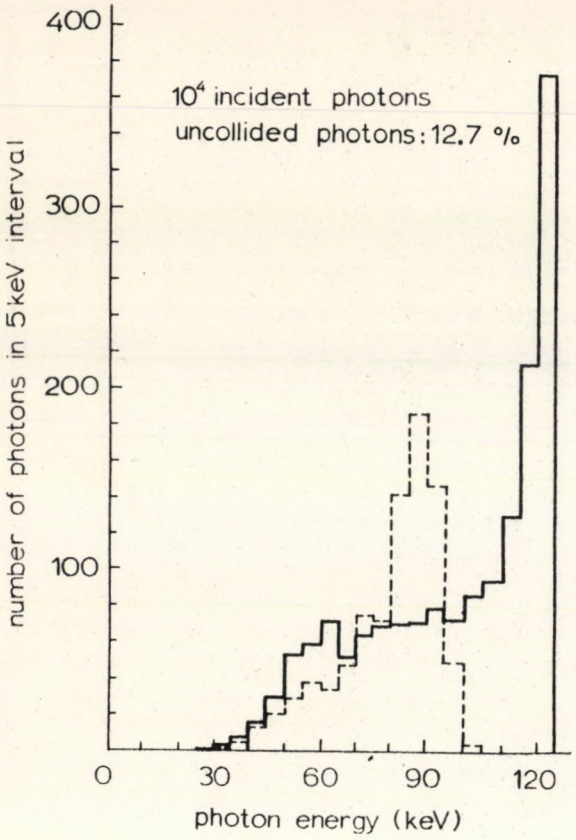

d/

Fig. 2

Spectra of the image-forming /full lines/ and backscattered /dashed lines/ photons for incident photon energies of /d/ 125 and /e/ 150 keV

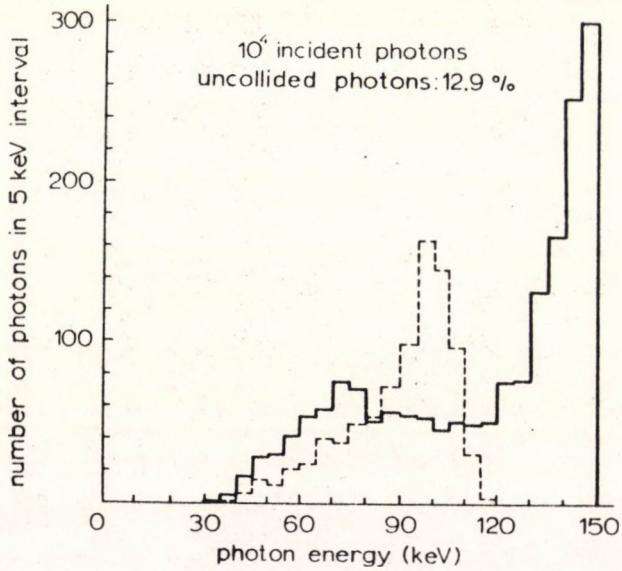

e/

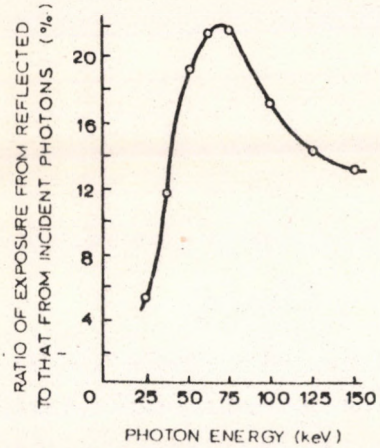

Fig. 3

The increase of exposure at the entry surface due to the backscattered photons

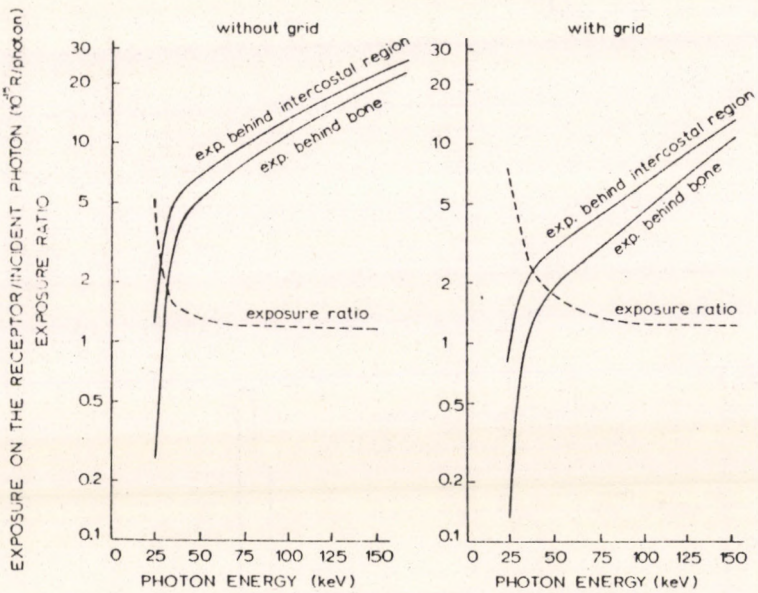

Fig. 4

Average exposures emerging on the two parts of the photoreceptor and their ratio vs. energy. /In the second graph the scattered photons are assumed to have been filtered out./

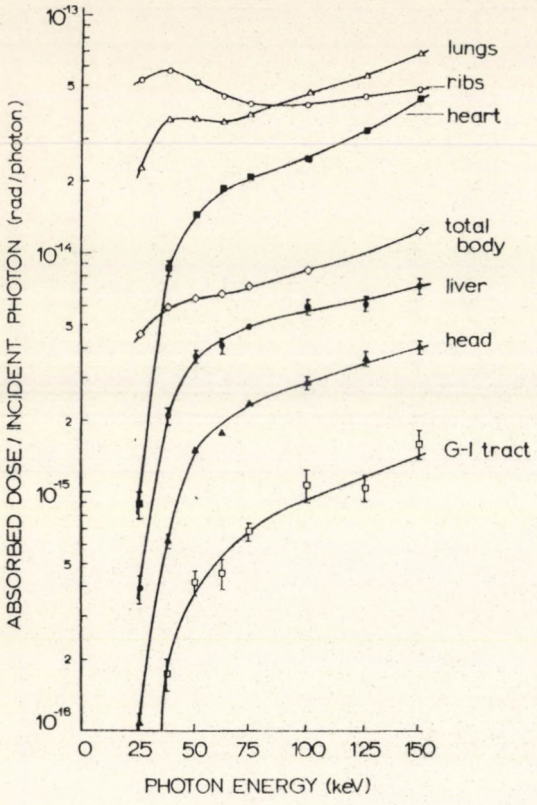

Fig. 5

Absorbed dose vs. incident photon energy

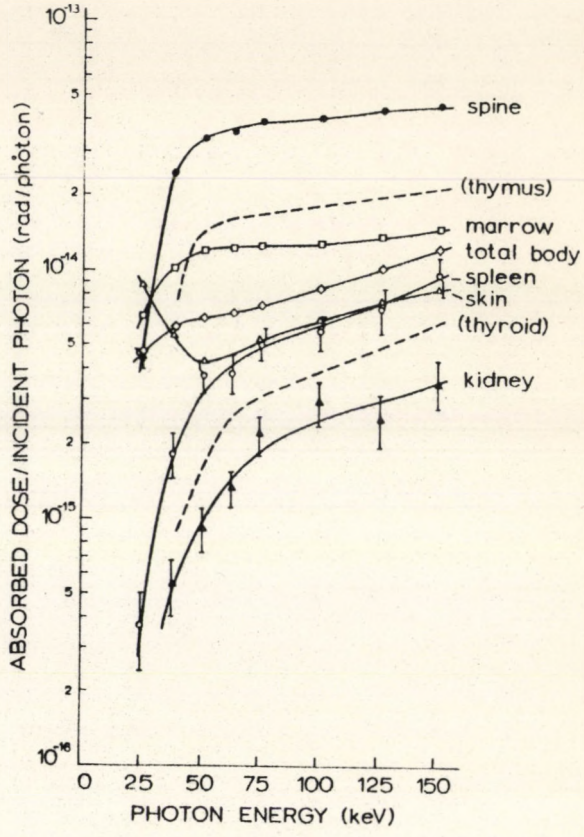

Fig. 6

Absorbed dose vs. incident photon energy

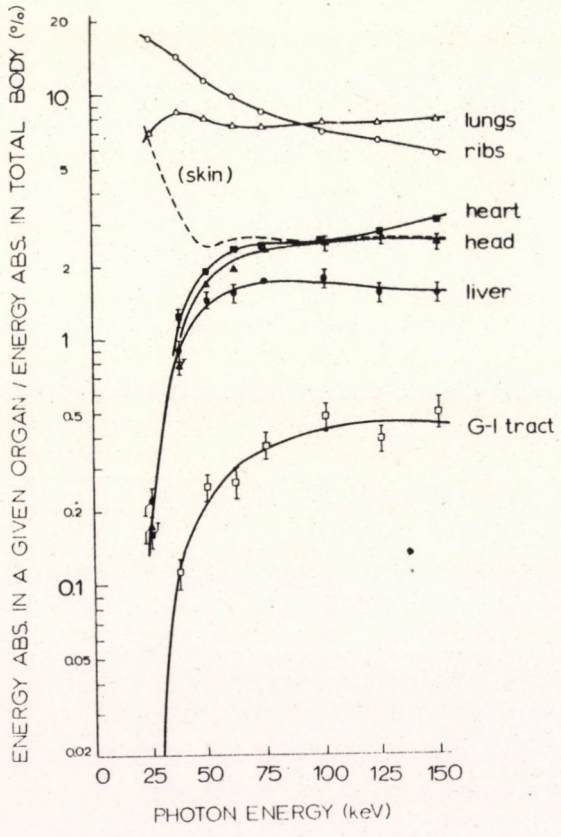

Fig. 7

The contribution of some parts of the body to the total energy absorption

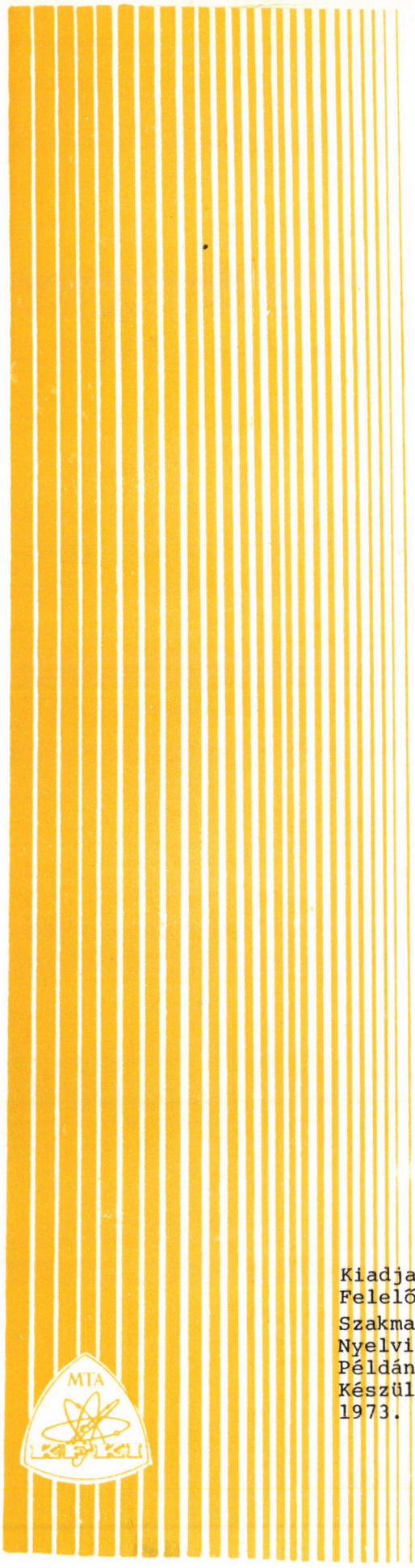

Kiadja a Központi Fizikai Kutató Intézet
Felelős kiadó: Szabó Ferenc igazgatóhelyettes
Szakmai lektor: Andrási Andor, Valkó János
Nyelvi lektor: T. Wilkinson
Példányszám: 225, Törzsszám: 73-8366
Készült a KFKI sokszorositó üzemében, Budapest,
1973. május hó